Available online at www.sciencedirect.com

SciVerse ScienceDirect

Ceramics International 38 (2012) 4875–4883

CERAMICS INTERNATIONAL

www.elsevier.com/locate/ceramint

Synthesis and characterization of the SBA-15/carbon cryogel nanocomposites

Biljana Babić [a,*], Maja Kokunešoski [a], Miroslav Miljković [b], Marija Prekajski [a], Branko Matović [a], Jelena Gulicovski [a], Dušan Bučevac [a]

[a] "Vinča" Institute of Nuclear Sciences, University of Belgrade, P.O. Box 522, 11000 Belgrade, Serbia
[b] Center of Electron Microscopy, Medical faculty, University of Niš, Serbia

Received 17 November 2011; received in revised form 25 February 2012; accepted 26 February 2012
Available online 5 March 2012

Abstract

The ordered mesoporous silica SBA-15 materials were synthesized using Pluronic P123 (non-ionic triblock copolymer, $EO_{20}PO_{70}O_{20}$), under acidic conditions. SBA-15/carbon cryogel composites were obtained by sol–gel polycondensation of resorcinol and formaldehyde followed by freeze drying, and subsequent pyrolysis, in the presence of different amounts of SBA-15. For comparison purpose, SBA-15/carbon composite was also prepared using sucrose as carbon source. These materials were characterized by room temperature nitrogen adsorption–desorption measurement, X-ray diffraction, scanning electron microscopy (SEM) and Fourier transform infrared (FT-IR) spectroscopy. It was revealed that the samples have amorphous structure, high specific surface area (350–520 $m^2\ g^{-1}$) and developed meso- as well as microporosity. The porosity of structure depends on the carbon source and Si/C ratio which can be easily controlled by varying concentration of starting solution.

Keywords: A. Sol–gel process; B. Nanocomposites; B. Porosity

1. Introduction

As soon as the mesoporous siliceous materials were synthesized [1–5], there has been an increasing interest in the tailoring of these materials for potential applications in separation and adsorption processes, catalysis, etc. One of the most studied mesoporous siliceous materials is SBA-15 (Santa Barbara No. 15), which can be synthesized in large quantities from tetraethyl orthosilicate (TEOS) in the presence of amphiphilic poly (alkylene oxide)-type triblock copolymers [6,7]. This amorphous material has a highly ordered mesoporous structure consisting of hexagonal nanochannels with diameter varying from 5 to 30 nm [8,9]. The pore size and the thickness of silica walls can be adjusted by varying the heating temperature and time of the reaction solution. Comprehensive studies on the SBA-15 structure have revealed certain amount of micropores, which connect neighboring mesopores (channels) [8–11].

Recent studies have showed that besides porosity, surface functionality strongly affects the properties and therefore efficiency of this kind of materials. It is especially true when it comes to applications of material as drug and gene carrier [12–15], for enzyme loading [16] and detection and adsorption of metal ions in living systems [17]. Despite such unique microstructure, the application of SBA-15 has some limitations due to low electronic conductivity and difficulty to incorporate functional groups on the surface of material. It is believed that these difficulties can be overcome by addition of carbon which possesses high electronic conductivity and a large amount of oxygen functional groups on the surface.

The composite of SBA-15 and porous carbon is a new class of material which possesses properties of both silica and carbon. Porous carbon materials have high electronic conductivity and high surface functionality whereas SBA-15 has well defined pore arrangement. These materials are also suitable for applications such as electromagnetic interference shielding or electromagnetic wave absorbing materials [18]. In addition, porous SBA-15/carbon composites are stable at high temperatures which make them suitable material for heat insulators, adsorbents or catalyst support.

* Corresponding author. Tel.: +381 11 3408224; fax: +381 11 3408224.
E-mail address: babicb@vinca.rs (B. Babić).

0272-8842/$36.00
doi:10.1016/j.ceramint.2012.02.078

Although a number of studies describe synthesis of mesoporous carbon-based materials using mesoporous silica as a template, the literature data about silica/carbon composites are still rare [18–25].

In this paper we have presented a completely new method for preparation of SBA-15/carbon cryogel composite. Carbon cryogel as a special class of porous carbon materials [26–30] was used as a source of carbon, for the first time. The carbon cryogel was obtained by sol–gel polycondensation of resorcinol and formaldehyde, followed by freeze drying, and subsequent pyrolysis. The results show that the advantage of using carbon cryogel is controllable, high specific surface area of obtained SBA-15/carbon composites.

New composite materials were characterized by XRD, SEM method and room temperature nitrogen adsorption. Special attention was dedicated to investigation of the specific surface and porosity of obtained samples, determined by BET method.

2. Experimental

2.1. Synthesis of SBA-15 samples

SBA-15 samples were synthesized first according to standard procedures [4,31], using Pluronic P123 (non-ionic triblock copolymer, $EO_{20}PO_{70}O_{20}$, BASF) as a surfactant and tetraethoxysilane (TEOS, 98%) as a source of silica. A 4 g sample of Pluronic P123 was dissolved in 30 ml of distilled water and 120 g of 2 M HCl solution and stirred for 1.5 h at 35 °C. The 8.5 g of TEOS was added dropwise into the solution and vigorously stirred at the same temperature for 1.5 h. This was followed by prolonged stirring and subsequent aging. Bearing in mind that the structure and surface properties of SBA-15 depend on time and temperature of aging [4] it is expected that the properties of SBA-15/carbon composite will be affected by these parameters as well. Therefore two different aging procedures were applied. According to the first one, which was proposed by Zhao et al. [4], the mixture was stirred at 35 °C for 20 h, and aged at 80 °C for 48 h (samples SBA-15/80). According to the second procedure [32], mixture was stirred at 35 °C for 22 h and aged at 100 °C for 24 h (samples SBA-15/100).

The final products obtained by both methods were filtered, washed with 600 ml of distilled water and dried at room temperature. Calcination was carried out in air by slowly increasing the temperature from room temperature to 500 °C. The heating rate was 1 °C/min. The holding time of 6 h was applied to decompose triblock copolymer.

2.2. Preparation of SBA-15/carbon cryogel composites

In the present work, resorcinol-formaldehyde (RF) gels with previously prepared SBA-15 were synthesized by polycondensation of resorcinol, ($C_6H_4(OH)_2$) (R), with formaldehyde, (HCHO) (F), according to the method proposed by Pekala [26]. Sodium carbonate (Na_2CO_3) (C), was used as a basic catalyst. RF solutions were prepared from resorcinol, 99% purity (E. Merck) and formaldehyde, 36% methanol stabilized (Fluka Chemie), sodium carbonate, p.a. quality (E. Merck), and distilled and deionized water (W). In all samples concentration of the starting solution was 20 wt.% and R/C ratio was 100.

Table 1
Synthesis conditions of SBA-15/carbon cryogel composites.

Sample	Weight of Si (g)	Weight of carbon (g)
Si80C 0.2	0.8	4.0
Si80C 0.5	2.0	4.0
Si80C 0.75	3.0	4.0
Si100C 0.2	0.8	4.0
Si100C 0.5	2.0	4.0
Si100C 1	4.0	4.0

Different amounts of SBA-15 were added in RF solutions. The volume of RF solution was calculated in order to yield 4 g of carbon. The synthesis conditions are listed in Table 1. The sample notation gives information about source of carbon, SBA-15 aging temperature and Si/C ratio in the sample. For instance: Si80C 0.2, means that SBA-15 was aged at 80 °C, source of carbon was carbon cryogel (C) and Si/C ratio was 0.2.

Suspensions were decanted in glass tubes (inner diameter = 10 mm) and sealed. In order to cause gelation, the tubes were placed 2 days at 25 °C, 1 day at 50 °C and finally 4 days at 85 °C.

RF cryogels with SBA-15 were prepared by freeze drying according to the procedure of Tamon et al. [27–30]. RF gels were immersed in a 10-times volume of t-butanol, p.a. quality (Centrohem-Beograd), for more than one day and rinsed to displace the liquid contained in the gels with t-butanol. The rinsing with t-butanol was repeated twice. The samples were prepared by freeze drying using Modulyo Freeze Dryer System Edwards, England, consisting of freeze dryer unit at High Vacuum Pump E 2 M 8 Edwards. Each sample was pre-frozen at −30 °C for 24 h. The frozen samples were dried in the acrylic chambers with shelves arrangements mounted directly on the top of the condenser of Freeze Dryer. The vacuum during 20 h long freeze drying was around 4 mbar.

SBA-15/carbon cryogel composites were prepared by carbonization of the samples in a conventional furnace, at 800 °C in nitrogen flow. After pyrolysis, the furnace was cooled to room temperature.

For the comparison, SBA-15/sucrose composites were prepared according to procedure from literature [33]. Briefly, 1 g of SBA-15/80 and SBA-15/100 was added to a solution obtained by dissolving 1.5 g of sucrose (BDH Prolabo) and 0.19 g of H_2SO_4 (p.a., Centrohem) in 5 ml of distilled water. The mixtures were heated for 6 h at 100 °C and for 6 h at 160 °C. After the addition of 1 g of sucrose, 0.1 g of H_2SO_4 and 5 ml of distilled water, the samples were treated again for 6 h at 100 °C and for 6 h at 160 °C. SBA-15/sucrose composites were prepared by carbonization of the samples in a conventional furnace, at 900 °C in nitrogen flow. After pyrolysis, the furnace was cooled to room temperature. The Si/C ratio in these samples was 0.5.

2.3. Characterization of SBA-15/carbon cryogel composites

Adsorption and desorption of N_2 were measured on SBA-15/carbon cryogel and SBA-15/sucrose composites at −196 °C using the gravimetric McBain method. From the obtained isotherms, the specific surface area, S_{BET}, pore size distribution, mesopore including external surface area, S_{meso}, and micropore volume, V_{mic}, of the samples were calculated. Pore size distribution was estimated by applying BJH method [34] to the desorption branch of isotherms whereas mesopore surface and micropore volume were estimated using the high-resolution α_s plot method [35–37]. Micropore surface, S_{mic}, was calculated by subtracting S_{meso} from S_{BET}.

SBA-15/carbon cryogel and SBA-15/sucrose composites were characterized by recording their powder X-ray diffraction (XRD) patterns on a Siemens D500 X-ray diffractometer using Cu Kα radiation with a Ni filter. The 2θ angular regions between 5° and 80° were explored at a scan rate of 1°/s with the angular resolution of 0.02° for all XRD tests.

For the Fourier transform infrared (FT-IR) spectroscopy analysis, the composites were mixed with KBr powder and pressed into pellets. FTIR spectra were measured on a Nicollet 380 FT-IR, Thermo Electron Corporation spectrometer in the spectral range from 400 to 4000 cm^{-1}, at room temperature.

The scanning electron microscopy (SEM) analysis was carried out on SBA-15/carbon cryogel and SBA-15/sucrose composites using the JEOL 6300F microscope.

Nitrogen adsorption isotherms on SBA-15/carbon and SBA-15/sucrose composites correspond to an evaluation of the nitrogen adsorption efficiency at room temperature.

3. Results and discussion

3.1. Adsorption isotherms – BET experiments

In our previous report [31], we showed that the isotherms for both SBA-15 samples are of type-IV, according to the IUPAC classification [38], and with a hysteresis loop associated with mesoporous materials. The specific surface areas, calculated by the BET equation, S_{BET}, were 710 $m^2\ g^{-1}$ for SBA-15/80 and 641 $m^2\ g^{-1}$ for SBA-15/100. For the SBA-15/80 sample, the pore radius varied between 2 and 6 nm while in the case of SBA-15/100 it varied between 2 and 25 nm, which means that the synthesis procedure at lower temperature (80 °C) gives samples with smaller pores, narrower pore size distribution and higher specific surface than those obtained by procedure at higher temperature (100 °C). The larger pore size in samples aged at higher temperature is explained to be the result of larger expansion of copolymer micelles at higher aging temperature [8,39]. These large micelles are expected to create large pores after calcination. In addition, it was also observed that the intermicellar attraction increases with temperature which leads to less dispersed Si precursor and therefore somewhat smaller specific surface than that of SBA-15 obtained at lower temperature [40]. Furthermore, the analysis of experimental data confirms the presence of micropores in both SBA-15 materials. The ratio of micro to mesopores is greater in the samples synthesized according to patent, i.e., aged at 100 °C for 24 h. The micro- to meso-pore ratio plays an important role especially when it comes to application such as adsorption of large molecules where the presence of mesopores is a prerequisite.

Adsorption and desorption isotherms of N_2 on the composite materials at −196 °C as a function of N_2 relative pressure are shown in Fig. 1. The isotherms for SBA-15/carbon cryogel composites are of type-IV and with a hysteresis loop associated with mesoporous materials. The considerable adsorption of nitrogen at low relative pressure indicates a presence of micropores in the samples. Unlike isotherms of SBA-15/carbon cryogel composites, the adsorption isotherms of Si80/sucrose and Si100/sucrose samples are of type I which is typical for microporous material. The isotherms display a low pressure hysteresis indicating that adsorbate is retained in micropores. The retained adsorbate persists after prolonged outgassing and can only be removed by pumping at elevated temperatures. These results clearly show that the samples obtained using sucrose as carbon source contain larger fraction of micropores. The comparison of Fig. 1a and b indicates that aging temperature of SBA-15 does not change the shape of isotherms in any significant way.

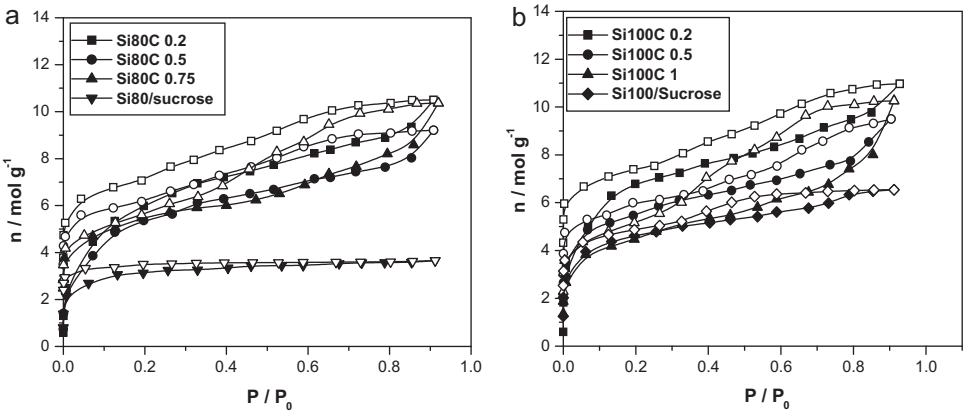

Fig. 1. Nitrogen adsorption and desorption isotherms, as a function of relative pressure of SBA-15/carbon cryogel and SBA-15/sucrose composite materials with different Si/C ratio and SBA-15 component aged at (a) 80 °C and (b) 100 °C. Solid symbols – adsorption, open symbols – desorption.

Table 2
Porous properties of starting SBA-15, SBA-15/carbon cryogel and SBA-15/sucrose composite materials.

Sample	S_{BET} ($m^2\ g^{-1}$)	S_{meso} ($m^2\ g^{-1}$)	S_{micro} ($m^2\ g^{-1}$)	S_{meso}/S_{micro}	V_{micro} ($cm^3\ g^{-1}$)
SBA-15/80	710	481	229	2.10	0.110
Si80C 0.2	471	118	353	0.33	0.200
Si80C 0.5	412	109	303	0.36	0.166
Si80C 0.75	431	167	264	0.63	0.126
Si80/sucrose	250	7	243	0.03	0.117
SBA-15/100	641	367	274	1.34	0.130
Si100C 0.2	519	95	424	0.22	0.235
Si100C 0.5	434	159	275	0.58	0.128
Si100C 1.0	350	206	144	1.43	0.064
Si100/sucrose	365	15	350	0.04	0.206

The specific surface and the pore structure parameters are listed in Table 2. As expected, the SBA-15/carbon composites exhibit a lower specific surface than starting SBA-15 materials due to silica framework shrinkage which occurs during carbonization. It can also be seen that the overall specific surface of the composite aged at 80 °C as well 100 °C depends on Si/C ratio. The decrease in specific surface with increasing Si/C ratio is considered to be due to the structural shrinkage of the silica framework during the carbonization of the carbon precursors. It was reported that carbon precursor undergoes considerable volume contraction during carbonization which creates compressive force on silica framework resulting in shrinkage of the silica structure [41–44]. Therefore it is expected that the presence of larger fraction of silica (SBA-15) causes lager shrinkage and thus smaller specific surface of the composite. Besides the effect of Si/C ratio on specific surface of the composite there is also effect of aging temperature, i.e., synthesis temperature of the silica on the specific surface. It is interesting to note that although the specific surface of SBA-15 aged at 100 °C is smaller than that of SBA-15 aged at 80 °C the specific surface of the composites containing SBA-15 aged at 100 °C and with 0.2 and 0.5 Si/C ratio is somewhat larger than that of composites containing SBA-15 aged at 80 °C. It is considered that the structural shrinkage which occurs during carbonization of the SBA-15/carbon composite is slightly smaller when synthesis temperature of SBA-15 is higher [40]. Consequently, the specific surface, S_{BET}, of the composites with SBA-15 aged at 100 °C (Si100C 0.2 and Si100C 0.5) is 20–50 $m^2\ g^{-1}$ larger than that for samples with SBA-15 aged at 80 °C (Si80C 0.2 and Si80C 0.5).

Generally, SBA-15/carbon cryogel samples have larger specific surfaces than SBA-15/sucrose composites. These results can be explained by the fact that carbon material obtained by carbonization of sucrose has smaller specific surface than that of material obtained by carbonization of cryogel. Therefore the overall specific surface of SBA-15/sucrose composites is lower than that of SBA-15/carbon cryogel.

The pore size distributions of the SBA-15/carbon cryogel and SBA-15/sucrose composite materials are shown in Fig. 2. All of the composites with carbon cryogel have developed micro- and mesoporosity with the pore radius below 5 nm. The Si80/sucrose and Si100/sucrose samples are microporous and mesoporosity is negligible.

The α_s plots, obtained using standard nitrogen adsorption isotherm, are shown in Fig. 3. The straight line in the high α_s region gives the mesoporous surface areas, which include the contribution of the external surface, S_{meso}, determined by its slope, while the micropore volume, V_{mic}, is given by the intercept. The calculated porosity parameters (S_{meso}, S_{mic}, V_{mic}) are shown in Table 2. Analysis of the experimental data confirms that in the composites with carbon cryogel a significant part of specific surface is in mesopores while composites with sucrose as

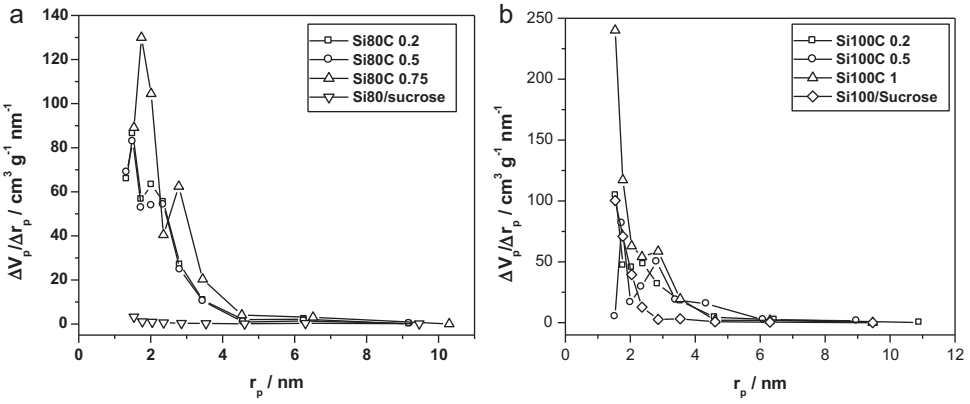

Fig. 2. Pore size distribution (PSD) for SBA-15/carbon cryogel and SBA-15/sucrose composite materials with different Si/C ratio and SBA-15 component aged at (a) 80 °C and (b) 100 °C.

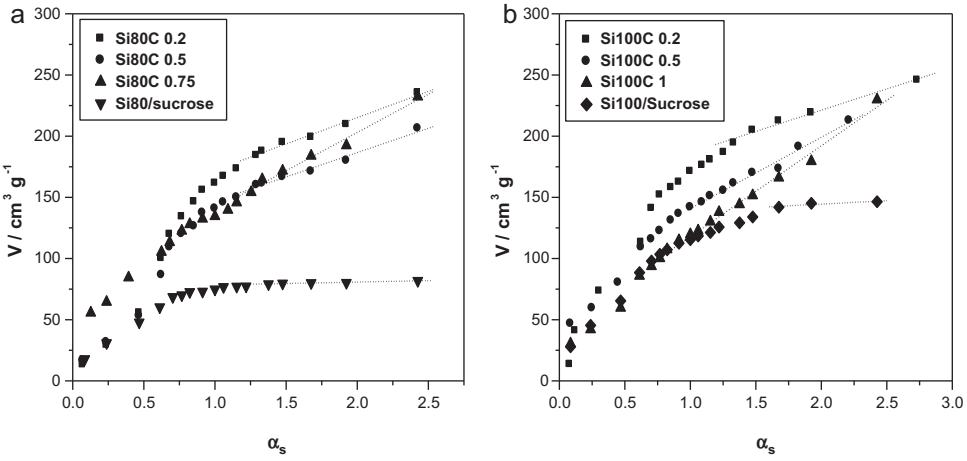

Fig. 3. α_s – plots of the nitrogen adsorption isotherms of SBA-15/carbon cryogel and SBA-15/sucrose composite materials with different Si/C ratio and SBA-15 component aged at (a) 80 °C and (b) 100 °C.

source of carbon are mostly microporous. Again, the presence of mesopores is essential for some applications, therefore the use of carbon cryogel as a source of carbon is an effective way to expand the scope of potential application of SBA-15/carbon composites.

With increasing the Si/C ratio in SBA-15/carbon composites the overall specific surface, S_{BET}, and microporous surface, S_{mic}, decrease while mesoporous surface, S_{meso}, increases. These results are in an agreement with previously made conclusion that the increase in Si/C ratio leads to an increase in shrinkage of SiO_2 framework during carbonization. Thus, it is expected that certain number of micropores simply disappears resulting in a decrease in microporous surface of obtained composites.

Fairly large microporosity in SBA-15/sucrose samples could be related to release of gaseous products during the conversation of sucrose into carbon. In the case of SBA-15/carbon cryogel composites, the porous network was established during the gelation process and that network was retained during the carbonization process.

It can be concluded that variation of synthesis temperature of SBA-15 as well as variation of Si/C ratio is an effective way to tailor properties of SBA-15/carbon composite.

3.2. XRD analysis

Fig. 4 shows the XRD patterns of the SBA-15/carbon cryogel and SBA-15/sucrose composite materials with different Si/C ratio and SBA-15 component aged at 80 °C and 100 °C. As can be seen, the patterns of all samples are quite similar. There are no well defined peaks, but just two broad humps which are typical for amorphous material. The larger hump, over the range from 15° to 31° 2θ (centered at 22.41° 2θ) is characteristic for amorphous silica [45,46] whereas the minor hump, over the range from 40° to 48° 2θ (centered at 43.01° 2θ) is characteristic for amorphous carbon [47]. The intensity of carbon hump is a function of the amount of carbon in sample, namely its intensity increases with decreasing Si/C ratio.

3.3. FT-IR analysis

FT-IR spectra of the SBA-15/carbon cryogel composite materials with different Si/C ratio and SBA-15 component aged at 100 °C are shown in Fig. 5. The spectra of the composites with Si/C ratio 1 and 0.5 exhibit two bands which are typical for SiO_2. The first one, at 800 cm^{-1}, refers to Si–O symmetric

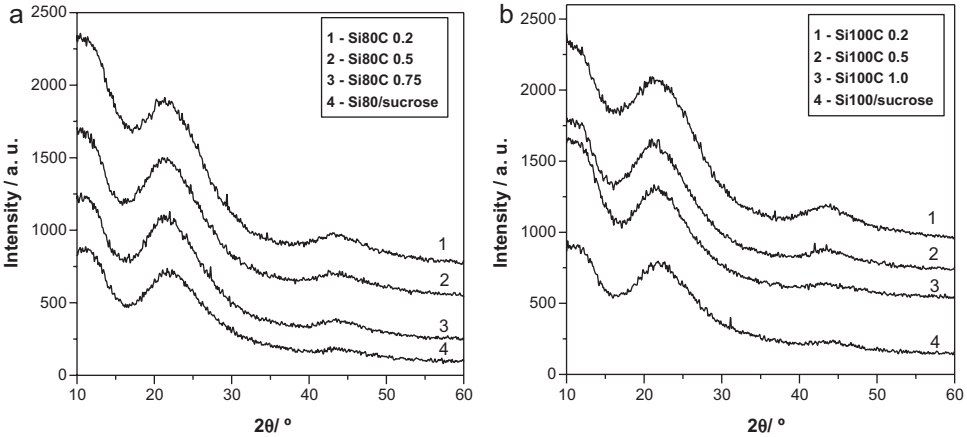

Fig. 4. X-ray diffraction (XRD) patterns of SBA-15/carbon cryogel and SBA-15/sucrose composite materials with different Si/C ratio and SBA-15 component aged at (a) 80 °C and (b) 100 °C.

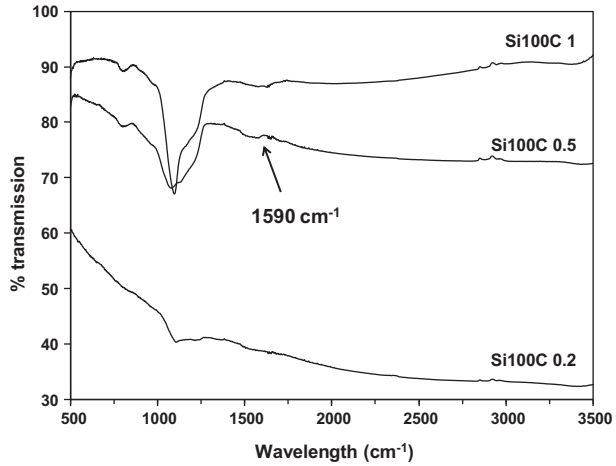

Fig. 5. FT-IR spectra of SBA-15/carbon cryogel composites with different Si/C ratio and SBA-15 component aged at 100 °C.

stretching, whereas the second one, at 1060 cm^{-1}, refers to Si–O asymmetric stretching [44]. Although the intensity of these bands decreases with a decrease of amount of SiO_2 (Si/C ratio) and they can be barely seen in sample with Si/C = 0.2, Fig. 5 confirms the presence of SBA-15 in the composites. Unlike SBA-15 spectra, carbon FT-IR spectra are difficult to obtain. Job et al. [48] reported that dried RF cryogels pyrolyzed at 800 °C show no absorption peaks. They have found that the infrared active groups disappear between 400 and 800 °C. However, it was also reported that the infrared band at about 1590 cm^{-1} appears after long grinding of carbon material [49]. Fig. 5 shows that this band was recorded in all samples. Although its intensity is fairly low it confirms the presence of carbon in the composites.

3.4. SEM analysis of SBA-15/carbon cryogel composites

SEM images of SBA-15/carbon cryogel and SBA-15/sucrose composites are shown in Figs. 6 and 7. Fig. 6 reveals images of composites obtained by using SBA-15/80 silica while Fig. 7 shows images of samples obtained by using SBA-15/100 silica. The images show that SBA-15/carbon cryogel composite samples consist of many peanut-like (SBA-15) domains of relatively uniform size (∼1 μm) which are aggregated into wheat-like structures surrounded by carbon particles. Similar structures of SBA-15 were reported in earlier papers [1,12,44]. As can be seen, the amount of graphite particles decreases as the Si/C ratio increases which implies that RF gel just partially penetrates into the mesopores of SBA-15. Therefore, the excess graphite, i.e., the graphite that cannot penetrate into silica pores, is located on the surface of peanut-like domains. Further support to this conclusion was found in preliminary, unpublished, results on chemical treatment of SBA-15/carbon composite by hydrofluoric acid which selectively dissolves SBA-15. Big pores, found after the treatment, indicate that RF gel did not penetrate into the core of SBA-15 domains. It is believed that polycondensation of resorcinol and formaldehyde and formation of RF clusters is fast reaction. The large size of

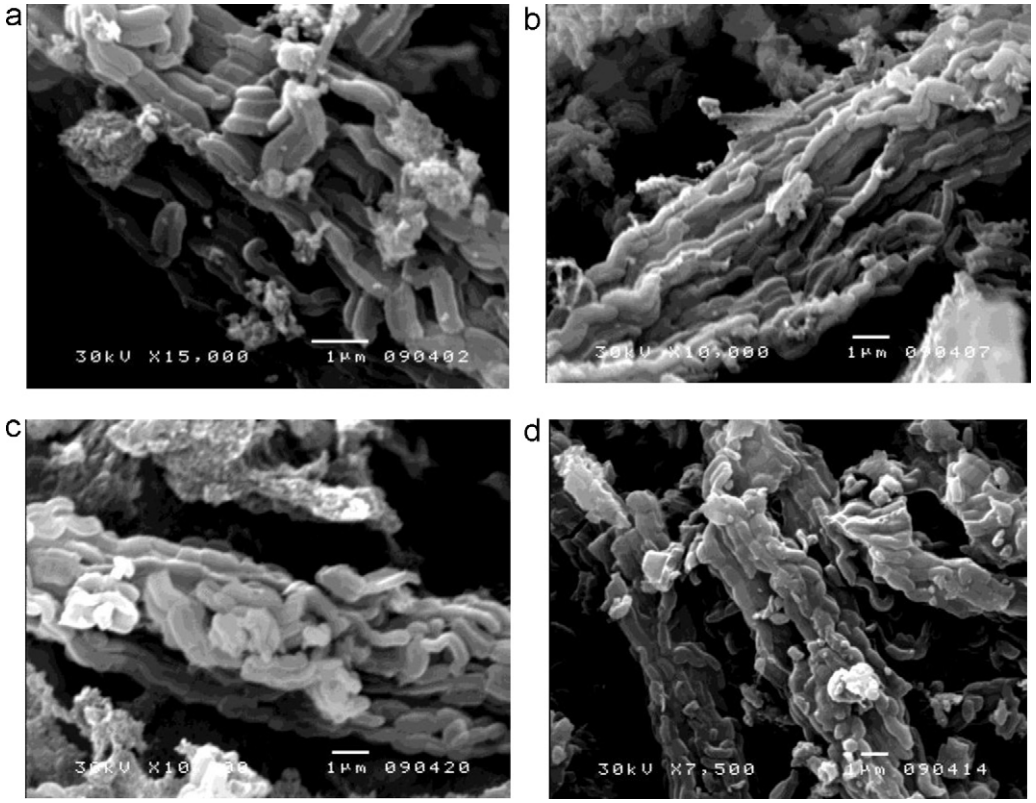

Fig. 6. SEM images of SBA-15/carbon cryogel and SBA-15/sucrose composite materials with different Si/C ratio and SBA-15 component aged at 80 °C: (a) Si80C 0.2, (b) Si80C 0.5, (c) Si80C 0.75 and (d) Si80/sucrose.

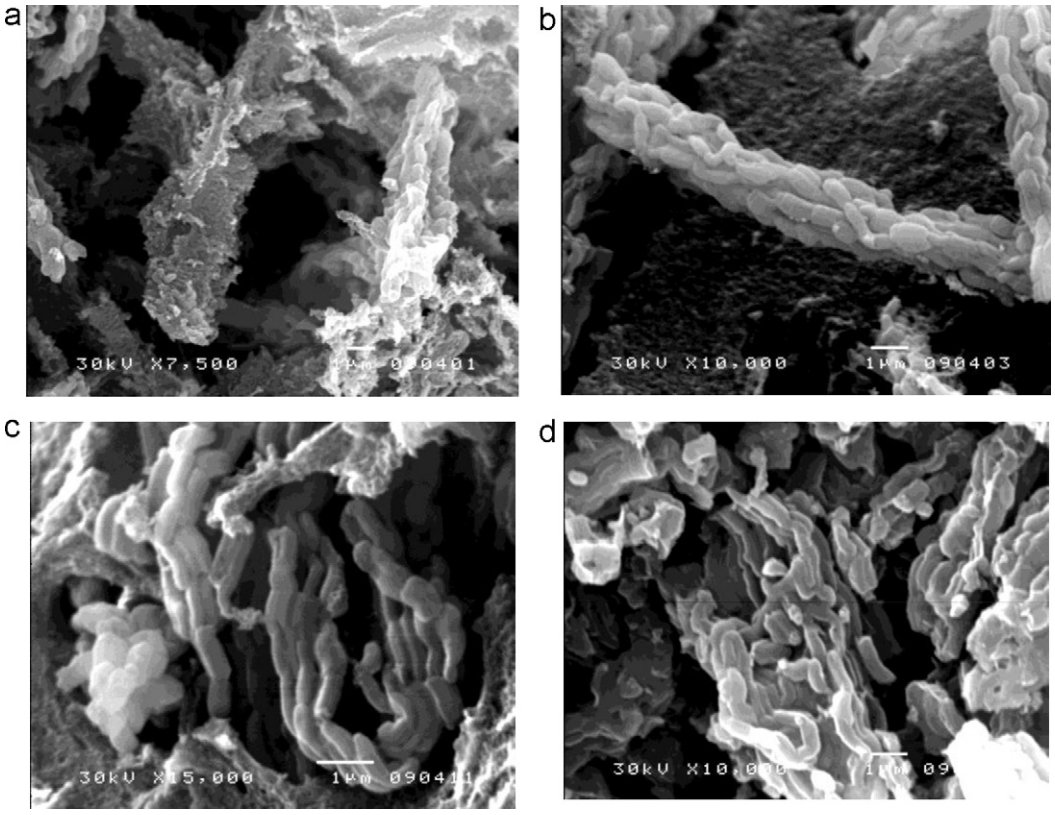

Fig. 7. SEM images of SBA-15/carbon cryogel and SBA-15/sucrose composite materials with different Si/C ratio and SBA-15 component aged at 100 °C: (a) Si100C 0.2, (b) Si100C 0.5, (c) Si100C 1.0 and (d) Si100/sucrose.

newly formed clusters actually prevents their penetration into the pores of SBA-15. On the contrary, aqueous solution of sucrose very easily fills the mesopores and almost all carbon goes into porous SBA-15. As Fig. 6d shows, there are no visible particles of carbon on the surface of peanut-like domains when sucrose was used as carbon source.

The comparison of images given in Figs. 6 and 7 reveals that the synthesis (aging) temperature of SBA-15 does not change the microstructure of the composites in any significant way.

Based on the presented SEM micrographs, it is believed that mechanical treatment of powder composite might change its specific surface. It is expected that crushing of wheat-like structures and reduction in the size of peanut-like (SBA-15) domains will be an effective way to further increase the specific surface of the composite.

3.5. Room temperature adsorption of nitrogen

Room temperature adsorption isotherms of nitrogen, as a function of relative pressure for several SBA-15/carbon cryogel and SBA-15/sucrose composite materials are shown at Fig. 8. The quantities of adsorbed nitrogen are in an agreement with

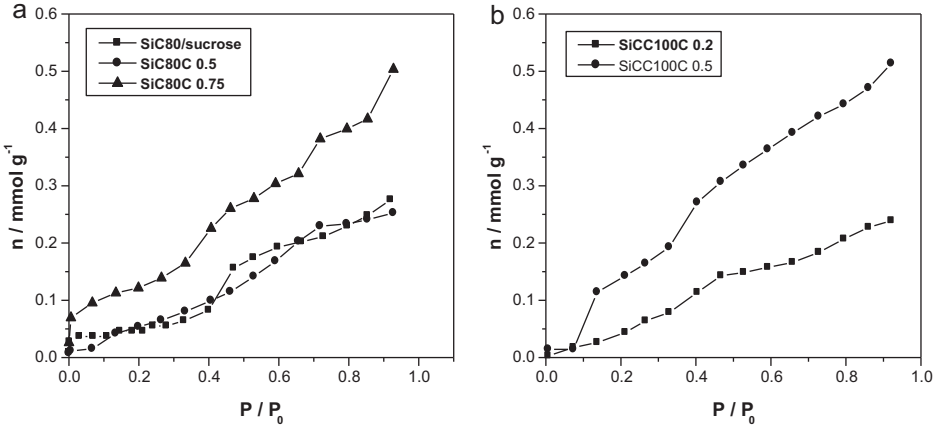

Fig. 8. Room temperature adsorption isotherms of nitrogen, as a function of relative pressure for SBA-15/carbon cryogel and SBA-15/sucrose composite materials with different Si/C ratio and SBA-15 component aged at (a) 80 °C and (b) 100 °C.

literature data for the carbon/silica composite synthesized from MCM-41 and polyfurfuryl alcohol [24]. The isotherms in Fig. 8 show that SBA-15/carbon cryogel composites, obtained from the different SBA-15 samples, but with very similar porous properties (Si80C 0.75 and Si100C 0.5) have adsorbed almost the same quantities of nitrogen at the same relative pressures. Also, the samples with higher amounts of mesopores are better adsorbents, i.e., the presence of mesopores increases the amount of adsorbed nitrogen. For comparison purpose, the adsorption isotherm for Si80/sucrose sample is presented as well. It is evident that SBA-15/carbon cryogel samples are as good as, or even better, adsorbents than Si80/sucrose composite.

4. Conclusion

The completely new method for preparation of SBA-15/carbon cryogel composite was presented. Silica/carbon cryogel composite materials have amorphous structure, high specific surface area (350–520 $m^2\,g^{-1}$) and developed meso- and microporosity. On the contrary, mesoporosity of silica/sucrose samples is negligible. The amount of micro- and mesopores in silica/carbon cryogel composites could be successfully controlled by Si/C ratio. The investigation of room temperature adsorption of nitrogen showed that the adsorbed quantities are function of the porous structure of the samples. The SBA-15/carbon composites are promising material for the application as adsorbents.

Acknowledgements

This paper has been supported by the Ministry of Science and Development, Republic of Serbia, under contract No. 45012.

References

[1] T. Yanagisawa, T. Shimizu, K. Kuroda, C. Kato, The preparation of alkyltriinethylaininonium–kaneinite complexes and their conversion to microporous materials, Bull. Chem. Soc. Jpn. 63 (1990) 988–992.
[2] J.S. Beck, J.C. Vartuli, W.J. Roth, M.E. Leonowicz, C.T. Kresge, K.D. Schmitt, C.T-W. Chu, D.H. Olson, E.W. Sheppard, S.B. McCullen, J.B. Higgins, J.L. Schlenkert, A new family of mesoporous molecular sieves prepared with liquid crystal templates, J. Am. Chem. Soc. 114 (1992) 10834–10843.
[3] B.G. Trewyn, I.I. Slowing, S. Giri, H.T. Chen, V.S.-Y. Lin, Synthesis and functionalization of a mesoporous silica nanoparticle based on the sol–gel process and applications in controlled release, Acc. Chem. Res. 40 (2007) 846–853.
[4] D. Zhao, J. Feng, Q. Huo, N. Melosh, G.H. Fredrickson, B.F. Chmelka, G.D. Stucky, Triblock copolymer syntheses of mesoporous silica with periodic 50 to 300 angstrom pores, Science 279 (1998) 548–552.
[5] D. Zhao, Q. Huo, J. Feng, B.F. Chmelka, G.D. Stucky, Nonionic triblock and star diblock copolymer and oligomeric surfactant syntheses of highly ordered, hydrothermally stable, mesoporous silica structures, J. Am. Chem. Soc. 120 (1998) 6024–6036.
[6] P. Yang, D. Zhao, D.I. Margolese, B.F. Chmelka, G.D. Stucky, Generalized syntheses of large-pore mesoporous metal oxides with semicrystalline frameworks, Nature 396 (1998) 152–155.
[7] P. Yang, D. Zhao, D.I. Margolese, B.F. Chmelka, G.D. Stucky, Block copolymer templating syntheses of mesoporous metal oxides with large ordering lengths and semicrystalline framework, Chem. Mater. 11 (1999) 2813–2826.
[8] M. Kruk, M. Jaroniec, Characterization of the porous structure of SBA-15, Chem. Mater. 12 (2000) 1961–1968.
[9] M. Imperior-Clerc, P. Davidson, A. Davidson, Existence of a microporous Corona around the mesopores of silica-based SBA-15 materials templated by triblock copolymers, J. Am. Chem. Soc. 122 (2000) 11925–11933.
[10] R. Ryoo, C.H. Ko, M. Kruk, V. Antoschshuk, M. Jaroniec, Block-copolymer-templated ordered mesoporous silica: array of uniform mesopores or mesopore–micropore network? J. Phys. Chem. B 104 (2000) 11465–11471.
[11] C.G. Sonwane, P.J. Ludovice, A note on micro- and mesopores in the walls of SBA-15 and hysteresis of adsorption isotherms, J. Mol. Catal. A: Chem. 238 (2005) 135–137.
[12] K. Lee, D. Lee, H. Lee, C.K. Kim, Z. Wu, K. Lee, Comparison of amine-functionalized mesoporous silica particles for ibuprofen delivery, Korean J. Chem. Eng. 27 (2010) 1333–1337.
[13] M. Valet-Regi, F. Balas, D. Arcos, Mesoporous materials for drug delivery, Angew. Chem. Int. Ed. 46 (2007) 7548–7558.
[14] M. Manzano, V. Aina, C.O. Arean, F. Balas, V. Cauda, M. Colilla, M.R. Delgado, M. Vallet-Regi, Studies on MCM-41 mesoporous silica for drug delivery: effect of particle morphology and amine functionalization, Chem. Eng. J. 137 (2008) 30–37.
[15] C.Y. Lai, B.G. Trewyn, D.M. Jeftinija, K. Jeftinija, S. Xu, S. Jeftinija, V.S.Y. Lin, A mesoporous silica nanosphere-based carrier system with chemically removable CdS nanoparticle caps for stimuli-responsive controlled release of neurotransmitters and drug molecules, J. Am. Chem. Soc. 125 (2003) 4451–4459.
[16] K. Nozawa, A. Shoji, M. Sugawara, Trypsin-loaded mesoporous silica as a sensing material for amplified detection of ATP4 – ions, Supramol. Chem. 22 (2010) 389–395.
[17] Q. Meng, X. Zhang, C. He, G. He, P. Zhou, C. Duan, Multifunctional mesoporous silica material used for detection and adsorption of Cu^{2+} in aqueous solution and biological applications in vitro and in vivo, Adv. Funct. Mater. 20 (2010) 1903–1909.
[18] J. Wang, C. Xiang, Q. Liu, Y. Pan, J. Guo, Ordered mesoporous carbon/fused silica composites, Adv. Funct. Mater. 18 (2008) 2995–3002.
[19] T. Grant Glover, K.I. Dunne, R.J. Davis, M. Douglas LeVan, Carbon–silica composite adsorbent: characterization and adsorption of light gases, Micropor. Mesopor. Mater. 111 (2008) 1–11.
[20] T. Grant Glover, M. Douglas LeVan, Carbon–silica composite adsorbent: sensitivity to synthesis conditions, Micropor. Mesopor. Mater. 118 (2009) 21–27.
[21] Y.H. Chu, M. Yamagishi, Z.M. Wang, H. Kanoh, T. Hirotsu, Adsorption characteristics of nanoporous carbon–silica composites synthesized from graphite oxide by a mechanochemical intercalation method, J. Colloid Interface Sci. 312 (2007) 186–192.
[22] Z. Wang, F. Li, N.S. Ergang, A. Stein, Synthesis of monolithic 3D ordered macroporous carbon/nano-silicon composites by diiodosilane decomposition, Carbon 46 (2008) 1702–1710.
[23] T. Yokoi, S. Seo, N. Chino, A. Shimojima, T. Okubo, Preparation of silica/carbon composites with uniform and well-ordered mesopores by esterification method, Micropor. Mesopor. Mater. 124 (2009) 123–130.
[24] H. Xu, H. Zhang, Y. Huang, Y. Wang, Porous carbon/silica composite monoliths derived from resorcinol–formaldehyde/TEOS, J. Non-Cryst. Solids 356 (2010) 971–976.
[25] P. Valle-Vigon, M. Sevilla, A.B. Fuertes, Mesostructured silica–carbon composites synthesized by employing surfactants as carbon source, Micropor. Mesopor. Mater. 134 (2010) 165–174.
[26] R.W. Pekala, Organic aerogels from the polycondensation of resorcinol with formaldehyde, J. Mater. Sci. 24 (1989) 3221–3227.
[27] H. Tamon, H. Ishizaka, T. Yamamoto, T. Suzuki, Preparation of mesoporous carbon by freeze drying, Carbon 37 (1999) 2049–2055.
[28] T. Yamamoto, T. Sugimoto, T. Suzuki, S.R. Mukai, H. Tamon, Preparation and characterization of carbon cryogel microspheres, Carbon 40 (2002) 1345–1351.
[29] H. Tamon, H. Ishizaka, T. Yamamoto, T. Suzuki, Influence of freeze-drying conditions on the mesoporosity of organic gels as carbon precursors, Carbon 38 (2000) 1099–1105.

[30] T. Yamamoto, T. Nishimura, T. Suzuki, H. Tamon, Control of mesoporosity of carbon gels prepared by sol–gel polycondensation and freeze drying, J. Non-Cryst. Solids 288 (2001) 46–55.
[31] M. Kokunešoski, J. Gulicovski, B. Matović, M. Logar, S.K. Milonjić, B. Babić, Synthesis and surface characterization of ordered mesoporous silica SBA-15, Mater. Chem. Phys. 124 (2010) 1248–1252.
[32] G.D. Stucky, B.F. Chmelka, D. Zhao, N. Melosh, Q. Huo, J. Feng, P. Yang, D. Pine, D. Margolese, W.Jr. Lukens, G.H. Fredrickson, P. Schmidt-Winkel, Block copolymer processing for mesostructured inorganic oxide materials, United State Patent, 6,592,764 (2003).
[33] S. Jun, S.H. Joo, R. Ryoo, M. Kruk, M. Jaroniec, Z. Liu, T. Ohsuna, O. Terasaki, Synthesis of new, nanoporous carbon with hexagonally ordered mesostructure, J. Am. Chem. Soc. 122 (2000) 10712–10713.
[34] E.P. Barret, L.G. Joyner, P.P. Halenda, The determination of pore volume and area distributions in porous substances. I. Computations from nitrogen isotherms, J. Am. Chem. Soc. 73 (1951) 373–380.
[35] K. Kaneko, C. Ishii, M. Ruike, H. Kuwabara, Origin of superhigh surface area and microcrystalline graphitic structures of activated carbons, Carbon 30 (1992) 1075–1088.
[36] M. Kruk, M. Jaroniec, K.P. Gadakaree, Nitrogen adsorption studies of novel synthetic active carbons, J. Colloid Interface Sci. 192 (1997) 250–256.
[37] K. Kaneko, C. Ishii, H. Kanoh, Y. Hanzawa, N. Setoyama, T. Suzuki, Characterization of porous carbons with high resolution α_s-analysis and low temperature magnetic susceptibility, Adv. Colloid Interface Sci. 76–77 (1998) 295–320.
[38] K.S.W. Sing, D.H. Everett, R.A.W. Haul, L. Moscou, R.A. Pierotti, J. Rouquerol, T. Siemieniewska, Reporting physisorption data for gas/solid systems with special reference to the determination of surface area and porosity, Pure Appl. Chem. 57 (1985) 603–619.
[39] E. Prouzet, T.J. Pinnavaia, You have full text access to this content, assembly of mesoporous molecular sieves containing wormhole motifs by a nonionic surfactant pathway: control of pore size by synthesis temperature, Angew. Chem. Int. Ed. 36 (1997) 516–518.
[40] A.B. Fuertes, Synthesis of ordered nanoporous carbons of tunable mesopore size by templating SBA-15 silica materials, Micropor. Mesopor. Mater. 67 (2004) 273–281.
[41] A.B. Fuertes, D.M. Nevskaia, Control of mesoporous structure of carbons synthesised using a mesostructured silica as template, Micropor. Mesopor. Mater. 62 (2003) 177–190.
[42] M. Kruk, M. Jaroniec, R. Ryoo, S.H. Joo, Characterization of ordered mesoporous carbons synthesized using MCM-48 silicas as templates, J. Phys. Chem. B 104 (2000) 7960–7968.
[43] S.H. Joo, R. Ryoo, M. Kruk, M. Jaroniec, Evidence for general nature of pore interconnectivity in 2-dimensional hexagonal mesoporous silicas prepared using block copolymer templates, J. Phys. Chem. B 106 (2002) 4640–4646.
[44] O.A. Anunziata, A.R. Beltramone, M.L. Martinez, L.L. Belon, Synthesis and characterization of SBA-3, SBA-15, and SBA-1 nanostructured catalytic materials, J. Colloid Interface Sci. 315 (2007) 184–190.
[45] C.E. Tambelli, J.F. Schneider, N.P. Hasparyk, P.J.M. Monteiro, Study of the structure of alkali–silica reaction gel by high-resolution NMR spectroscopy, J. Non-Cryst. Solids 352 (2006) 3429–3436.
[46] E.V. Hoek, R. Winter, Amorphous silica and the intergranular structure of nanocrystalline silica, Phys. Chem. Glasses 43C (2002) 80–84.
[47] C. Adelhelm, M. Balden, M. Rinke, M. Stueber, Influence of doping (Ti, V, Zr, W) and annealing on the sp2 carbon structure of amorphous carbon films, J. Appl. Phys. 105 (2009) 33522–33531.
[48] N. Job, R. Pirard, J. Marien, J.P. Pirard, Porous carbon xerogels with texture tailored by pH control during sol–gel process, Carbon 42 (3) (2004) 619–628.
[49] B. Dou, J. Li, Y. Wang, H. Wang, C. Ma, Z. Hao, Adsorption and desorption performance of benzene over hierarchically structured carbon–silica aerogel composites, J. Hazard. Mater. 196 (2011) 194–200.